Journal of Trace Elements in Medicine and Biology 79 (2023) 127208

Contents lists available at ScienceDirect

Journal of Trace Elements in Medicine and Biology

journal homepage: www.elsevier.com/locate/jtemb

Integrated insight into the molecular mechanisms of selenium-modulated, MPP^+-induced cytotoxicity in a Parkinson's disease model

Wen Liu [a,1], Feiyang Zhang [a,1], Wu Liang [b,1], Kaixin Huang [a], Chenguang Jia [a], Jie Zhang [a], Xiang Li [a,c], Wei Wei [a,c,*], Rui Gong [a,**], Jincao Chen [a,**]

[a] Department of Neurosurgery, Zhongnan Hospital, Wuhan University, Donghu Road 169, Wuhan 430071, China
[b] Department of Neurosurgery, Minda Hospital of Hubei Minzu University, Enshi 445000, China
[c] Neuroepigenetic Research Lab, Medical Research Institute, Wuhan University, Donghu Road 115, Wuhan 430071, China

ARTICLE INFO

Keywords:
Parkinson's disease
Selenium
RNA-seq
MRNA
LncRNA

ABSTRACT

Objective: Parkinson's disease (PD) is a neurodegenerative disease that is associated with oxidative stress. Due to the anti-inflammatory and antioxidant functions of Selenium (Se), this molecule may have neuroprotective functions in PD; however, the involvement of Se in such a protective function is unclear.

Methods: 1-methyl-4-phenylpyridinium (MPP^+), which inhibits mitochondrial respiration, is generally used to produce a reliable cellular model of PD. In this study, a MPP^+-induced PD model was used to test if Se could modulate cytotoxicity, and we further capture gene expression profiles following PC12 cell treatment with MPP^+ with or without Se by genome wide high-throughput sequencing.

Results: We identified 351 differentially expressed genes (DEGs) and 14 differentially expressed long non-coding RNAs (DELs) in MPP^+-treated cells when compared to controls. We further document 244 DEGs and 27 DELs in cells treated with MPP^+ and Se vs. cells treated with MPP^+ only. Functional annotation analysis of DEGs and DELs revealed that these groups were enriched in genes that respond to reactive oxygen species (ROS), metabolic processes, and mitochondrial control of apoptosis. Thioredoxin reductase 1 (Txnrd1) was also identified as a biomarker of Se treatment.

Conclusions: Our data suggests that the DEGs Txnrd1, Siglec1 and Klf2, and the DEL AABR07044454.1 which we hypothesize to function in *cis* on the target gene Cdkn1a, may modulate the underlying neurodegenerative process, and act a protective function in the PC12 cell PD model. This study further systematically demonstrated that mRNAs and lncRNAs induced by Se are involved in neuroprotection in PD, and provides novel insight into how Se modulates cytotoxicity in the MPP^+-induced PD model.

1. Introduction

Parkinson's disease (PD) is a common neurodegenerative disorder characterized by static tremors, bradykinesia, rigidity, and impaired balance [1]. The pathogenesis of PD appears to result from the complex interaction of aberrant protein aggregation, mitochondrial dysfunction, oxidative stress, impairments of lysosome-autophagy systems, and neuroinflammation [2]. Collectively, these dysfunctions lead to accelerated loss of dopaminergic neurons. To date, the progression of PD cannot be prevented, and current therapies principally focus on symptomatic treatment [3]. Thus, there is an urgent need to identify effective therapeutic approaches to treat PD or postpone PD progression.

Selenium (Se), an essential trace element and has a wide range of biological functions including the induction of active thyroid hormone,

Abbreviations: PD, Parkinson's disease; Se, selenium; GPx, glutathione peroxidase; Selenos, selenoprotein S; Selenoh, selenoprotein H; Selenow, selenoprotein W; Selenoo, selenoprotein O; Sephs2, selenophosphate synthetase 2; Txnrd1, thioredoxin reductase 1; Txnrd 2, thioredoxin reductase 2; Txnrd 3, thioredoxin reductase 3; lncRNA, long noncoding RNA; MPP^+, 1-methyl-4-phenylpyridinium; DEG, differential expression of gene; DEL, differential expression of lncRNA; CCK-8, cell counting kit-8 assay; ROS, reactive oxygen species; siglec1, sialoadhesin; Klf2, krueppel-like factor 2; Cdkn1a, Cyclin-dependent kinase inhibitor 1; FDR, false discovery rate; GO, Gene Ontology; KEGG, Kyoto Encyclopedia of Genes and Genomes.

* Corresponding author at: Department of Neurosurgery, Zhongnan Hospital, Wuhan University, Donghu Road 169, Wuhan 430071, China
** Corresponding authors.
E-mail addresses: wei.wei@whu.edu.cn (W. Wei), gongruia@126.com (R. Gong), chenjincao2012@163.com (J. Chen).
[1] These authors contributed the study equally

https://doi.org/10.1016/j.jtemb.2023.127208
Received 3 November 2021; Received in revised form 13 June 2022; Accepted 17 May 2023
Available online 24 May 2023

antioxidant defense systems, and immune function [4]. Se exists as a component of selenoproteins, most of which are oxidoreductases involved in resisting oxidative stress [4–6]. In Alzheimer's disease, selenoproteins enhance antioxidant capacity, mitigate Aβ and tau pathology, reverse synaptic deficits, and ameliorate cognitive decline [7]. In PD, due to pathogenetic mechanisms of oxidative stress and mitochondrial dysfunction, it has been suggested that Se has a neuroprotective role and several studies have documented that Se contributes to slower PD disease progression [8–10]. Recently, multiple studies suggested dietary Se could modulate locomotor activity and reduce dopaminergic neurons in PD animal models [11,12]. Of note, Se deficiency leads to vulnerability in dopaminergic neurons [12], and dietary Se may reduce DNA damage and reverse striatal dopamine depletion [11,13]. Moreover, selenoproteins play an essential role in protecting against PD following exposure to certain environmental neurotoxins [14–16]; however, the association between Se and PD remains unclear.

Transcriptomic alterations have been documented following exposure to Se [17,18]. Se supplementation may induce the expression of selenoproteins, such as glutathione peroxidase 1 (GPx1), glutathione peroxidase 4 (GPx4), selenoprotein S (selenoS) and thioredoxin reductase 2 (Txnrd 2) [17]. Alternatively, Se may modify expression of genes involved in innate immunity and stress response [18] and, similarly, Se may alter the expression of long noncoding RNAs (lncRNAs). In a chicken model, Se deficiency has been proven to induce reduction in lncRNA-3215, resulting in calcium disorders within the heart [19]. Following treatment of breast cancer cells with Se, 28 lncRNAs were found to be differentially expressed [20]. Furthermore, during PD-associated neuroinflammation, Se treatment can alter the expression of glutathione-associated enzymes [21]. Evidence further indicates the protective effect of Se in PD, but the underlying mechanisms await further investigation.

To explore the protective function of Se in PD, we employed a common PD model system. Specifically, 1-methyl-4-phenylpyridinium (MPP^+), which is selectively absorbed by dopaminergic neurons, accumulates in the mitochondria. MPP^+ subsequently inhibits complex I of the mitochondrial electron transport chain, and this feature of MPP^+ partly recapitulates the pathogenesis of PD [22]. PC12 cells provide a catecholamine cell culture model for screening environmental agents associated with idiopathic PD [23]. In the present study, we used MPP^+ treatment of PC12 as a cellular model for PD [23,24]. Using this model, we confirmed that Se could modulate MPP^+-induced cytotoxicity. Differential gene expression and gene function analysis were performed using RNA sequencing in normal PC12 cells, MPP^+-treated PC12 cells, and PC12 cells treated with a combination of Se and MPP^+. The aim of this study was to examine the functional role of differentially expressed genes (DEGs) and lncRNAs (DELs) in this Se-treatment PD model to uncover genes and lncRNAs have neuroprotective functions in PD.

2. Materials and methods

2.1. Cell culture

The rat pheochromocytoma cell line PC12 (Procell Life Science & Technology, Wuhan, China) was grown in RPMI 1640 medium supplemented with 5% fetal bovine serum and 5% horse serum (Gibco, Australia), and cells were incubated in a 5% CO^2, 37 °C atmosphere. For differentiation, cells were cultured in RPMI 1640 medium, containing 10% fetal bovine serum and 100 ng/ml nerve growth factor (Sigma-Aldrich, St. Louis, USA) for 5 days. Differentiated PC12 cells were subsequently cultured in normal growth medium and were used in subsequent experiments. Where indicated, growth medium was replaced with serum-free RPMI 1640 with or without various concentrations (2, 5, 10, 20 and 40 μM) of Na_2SeO_3 (Sigma). Differentiated PC12 cells were incubated with Se for 48 h.

Following Se treatment, differentiated PC12 cells were cultured in serum-free medium for an additional 24 h and, subsequently, this medium was replaced with serum-free RPMI 1640 medium with or without various concentrations (500, 1000, 1500 and 3000 μM) of MPP^+ (Sigma) for 24 h. The optimal concentration for combination Se/MPP^+ treatment was carefully chosen by exposing PC12 cells to both compounds. For RNA sequencing experiments, the control group cells were cultured in serum-free medium for 48 h. In the MPP^+ group, PC12 cells were cultured in serum-free medium for 24 h, then incubated with MPP^+ (1500 μM) for 24 h. In the combination Se/MPP^+ group, PC12 cells were exposed to Se (20 μM) for 24 h, then incubated with MPP^+ (1500 μM) for an additional 24 h.

2.2. Cell toxicity assay

Cell toxicity was determined using the Cell Counting Kit-8 assay (CCK-8) (Vazyme, Nanjing, China) according to the manufacturer's instructions. In brief, an equal number of PC12 cells were seeded into 96-well plates, and subsequently treated both Se and/or MPP^+ as described above. At the end of treatment, each well was incubated with 10 μL CCK-8 solution for 1 h and then the absorbance of each well was read at 490 nm using a spectrophotometer.

2.3. RNA isolation, library construction and sequencing

Total RNA was extracted from untreated (control) PC12 cells, and cells treated with MPP^+ (1500 μM) or a combination of Se (20 μM) and MPP^+ (1500 μM) using TRIzol reagent (Invitrogen, Carlsbad, CA, USA). In each treatment group, three independent samples were collected. RNA purity and concentration was determined using a Nano Photometer® spectrophotometer (IMPLEN, Westlake Village, CA, USA) and Qubit® RNA Assay kits (Thermo Fisher Scientific, Waltham, MA, USA). In addition, RNA integrity and quantity were assessed using a RNA Nano 6000 LabChip Kit and a Bioanalyzer 2100 (Agilent Technologies, Santa Clara, CA, USA). Using this assay system, RNA integrity number (RIN) values were found to be greater than nine indicating strong RNA integrity.

One microgram of total RNA was used to deplete ribosomal RNA using the Ribo-off rRNA Depletion Kit (Vazyme). Subsequently, this RNA was used for first-strand cDNA synthesis by reverse transcription. cDNA libraries were constructed by following instructions provided with the VAHTS® Universal V8 RNA-seq Library Prep Kit for Illumina sequencing (Vazyme Biotech). Libraries were subsequently sequenced using a NovaSeq 6000 sequencer (Illumina, San Diego, CA, USA).

2.4. Quality control and transcriptome assembly

Results from high-throughput sequencing data were converted using bcl2fastq into raw sequencing reads. These raw reads were filtered by removing adapter-contamination reads, low-quality reads ($>$ 50% nucleotides with $Q \leq 19$), and reads with $>$ 5% poly-N. The Q30 value, indicative of base sequencing error rate, was calculated at $<$ 0.1%. Following these steps, this filtered data was subsequently used for the downstream analyses.

Gene references files in fasta and gtf formats were downloaded from ENSEMBL (code: wget http://ftp.ensembl.org/pub/release-89/fasta/rattus_norvegicus/dna/Rattus_norvegicus.Rnor_6.0.dna.toplevel.fa.gz). We used HISAT2 (v2.2.1) to build indexes from fasta files. HISAT2 (v2.2.1) alignment was then applied to map reads for indexing. Samtools (v1.8) was used to convert sam files to bam files along with conducting file sorting. To quantify expression at the gene level, we used HTseq-count (v0.13.5). These files were then imported to R studio Server for further analysis.

2.5. DEG identification and enrichment analysis

DEGs were identified using DESeq2 (v1.30.1) to analyze raw counts. Significant genes were defined as genes with fold change $>$ 2 and a false

discovery rate (FDR) (Benjamini/Hochberg correction method) of < 0.05, which were later categorized as "up" and "down". We applied Gene Ontology (GO) [25] and Kyoto Encyclopedia of Genes and Genomes (KEGG) [26] analysis of DEGs using R package ClusterProfiler (v3.18.1). Overlapping of "up" and "down" between MPP^+ group vs. controls, and combination Se/MPP^+ vs. the MPP^+-only group were investigated to obtain key DEGs in these two experimental groups.

2.6. lncRNA quantification and DELs identification

As the genome of *Rattus norvegicus* has been well annotated, we identified lncRNAs from gtf files containing all lncRNA transcripts rather than using of de novo identification. Gtf files are acquired from ENSEMBL (http://ftp.ensembl.org/pub/release-89/gtf/rattus_norvegicus/Rattus_norvegicus.Rnor_6.0.89.gtf.gz). The original gtf file was later filtered using transcript biotype of lncRNA, antisense, retained_intron and sense_intronic [27]. Fastq files were aligned with HISAT2 (v2.2.1) to the filtered gtf files, followed by importing to Samtools (v1.8) to obtain sorted bam files. Quantification was employed using FeatureCounts (v2.0.1) at the transcript level as certain genes may contain transcripts of both mRNAs and non-coding RNAs. DELs were identified using the DEseq2 R package (v1.30.1). To be considered significant, DELs were required to meet a threshold with a fold change more than 2 and FDR (Benjamini/Hochberg correction method) less than 0.1 based on the negative binomial distribution model.

2.7. lncRNA target genes identification and function annotation

lncRNA target genes were screened out as 50 kb upstream or 50 kb downstream of the source lncRNA locus, to identify potential lncRNA *cis*-element target genes. To fully understand the potential function of such target genes, GO category analysis and KEGG pathway analysis was applied using R package clusterProfiler (v3.18.1). R packages ggplot2 (v3.3.5), pheatmap (v1.0.12), dplyr (v1.0.6), stringr (v1.4.0), rtracklayer (v1.50.0) were employed for data processing and plotting.

2.8. Quantitative real-time RT-PCR

We randomly selected five key DEGs (Col6a3, Gadd45b, Klf2, Pdk4 and Gpr37) and used these for validation of the sequencing results by quantitative real-time PCR (RT-qPCR). Primers were designed using NCBI Primer-BLAST (Supplementary Table 5). β-actin was used as the internal quantitative reference. Genomic DNA was depleted in total RNA preparations prior to RT-qPCR analysis, and cDNA was synthesized using PrimeScript™ RT reagent Kit (TaKaRa, Dalian, China). RT-qPCR was subsequently performed per the instructions of ChamQ Universal SYBR qPCR Master Mix (Vazyme). Relative gene was analyzed using the $2^{-\Delta\Delta Ct}$ method.

2.9. Statistical analysis

All data were expressed as mean ± standard error of mean ($\bar{x}$ ± SEM). One-way ANOVA followed by Bonferroni's multiple comparison test was used for data comparison by using GraphPad Prism version 9.0 (San Diego, CA, USA). Values of $P < 0.05$ were considered statistically significant.

3. Result

3.1. Supplementation of Se prevents MPP^+ induced neuronal cell death

We performed a CCK-8 assay to investigate the toxicity of MPP^+ in PC12 cells. Cells were treated with 0, 500, 1000, 1500 and 3000 μM MPP^+ for 24 h. Cell viability following exposure to MPP^+ revealed a significant decrease when MPP^+ concentration increased from 500 to 3000 μM when compared with the untreated control cells (Fig. 1A). Similarly, cell viability of PC12 cells exposed to different concentrations of Se (2, 5, 10, 20 and 40 μM) was also assessed using the CCK-8 assay. Compared to untreated controls, cell viability showed no statistical difference following exposure to 2–40 μM Se (Fig. 1B).

MPP^+ induces a significant and steady loss of viability in neuronal cells exposed to concentration of 1500 μM, which is the optimum concentration for assessing the protective function of Se in our PD model. Therefore, we chose 1500 μM MPP^+ for further studies. To determine Se ability to modulate MPP^+-induced cytotoxicity, we incubated PC12 cells with both Se (2, 5, 10, 20 and 40 μM) and MPP^+ (1500 μM) (Fig. 1C). Cell viability assays showed that Se, especially cells treated with 20 μM Se, significantly reduced MPP^+-induced cell death. These results indicated that Se could protect PC12 cells against MPP^+-induced neuronal death.

3.2. Characterization of DEGs and DELs by RNA-seq

To systematically investigate the protective mechanisms and pathways activated by Se, we extracted total RNA from untreated control PC12 cells, MPP^+ (1500 μM) treated PC12 cells, and combination Se (20 μM) and MPP^+ (1500 μM) treated PC12 cells. Subsequently, cDNA libraries were constructed following ribosomal RNA depletion and

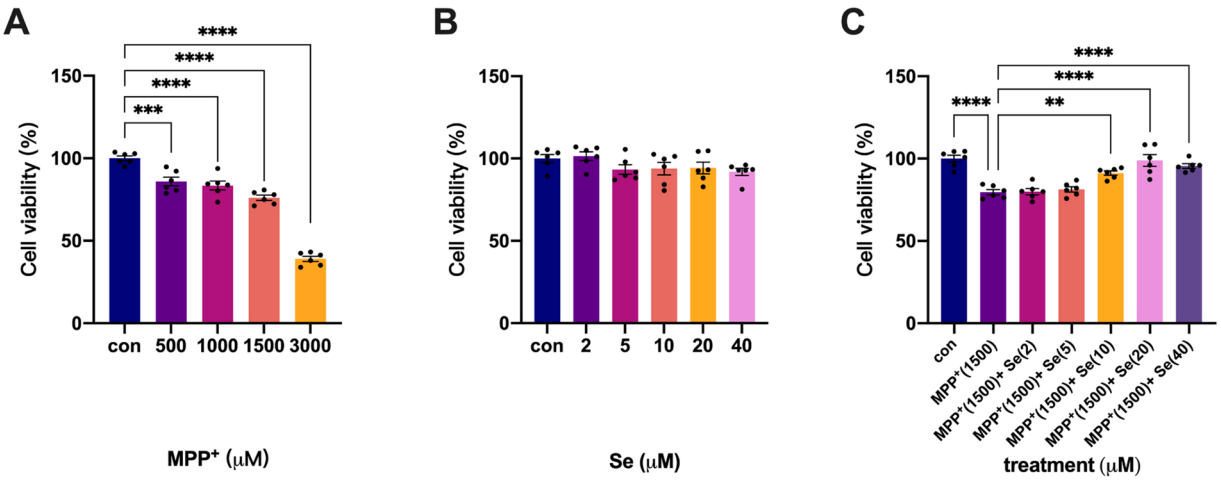

Fig. 1. Cell viability of PC12 cells cultured in serum-free RPMI 1640 medium with or without various concentrations (500, 1000, 1500 and 3000 μM) of MPP^+ (A), with or without various concentrations (2, 5, 10, 20 and 40 μM) of Se (B) and with Se (0–40 μM) + MPP^+ (1500 μM) or without both reagents (C). Error bars indicate mean ± SEM (n = 6). *p < 0.05, * *p < 0.01, * **p < 0.001 and * ** *p < 0.0001.

sequenced using a NovaSeq 6000 apparatus (Fig. 2A). In addition, to clearly demonstrated the Se status in PC12 cells, intracellular Se concentrations in the control group, MPP^+ group, and Se/MPP^+ group were measured by inductively-coupled plasma mass spectrometry. The results showed that the combination Se/MPP^+ group had significant higher intracellular Se concentrations than the other two groups (Fig. 2B).

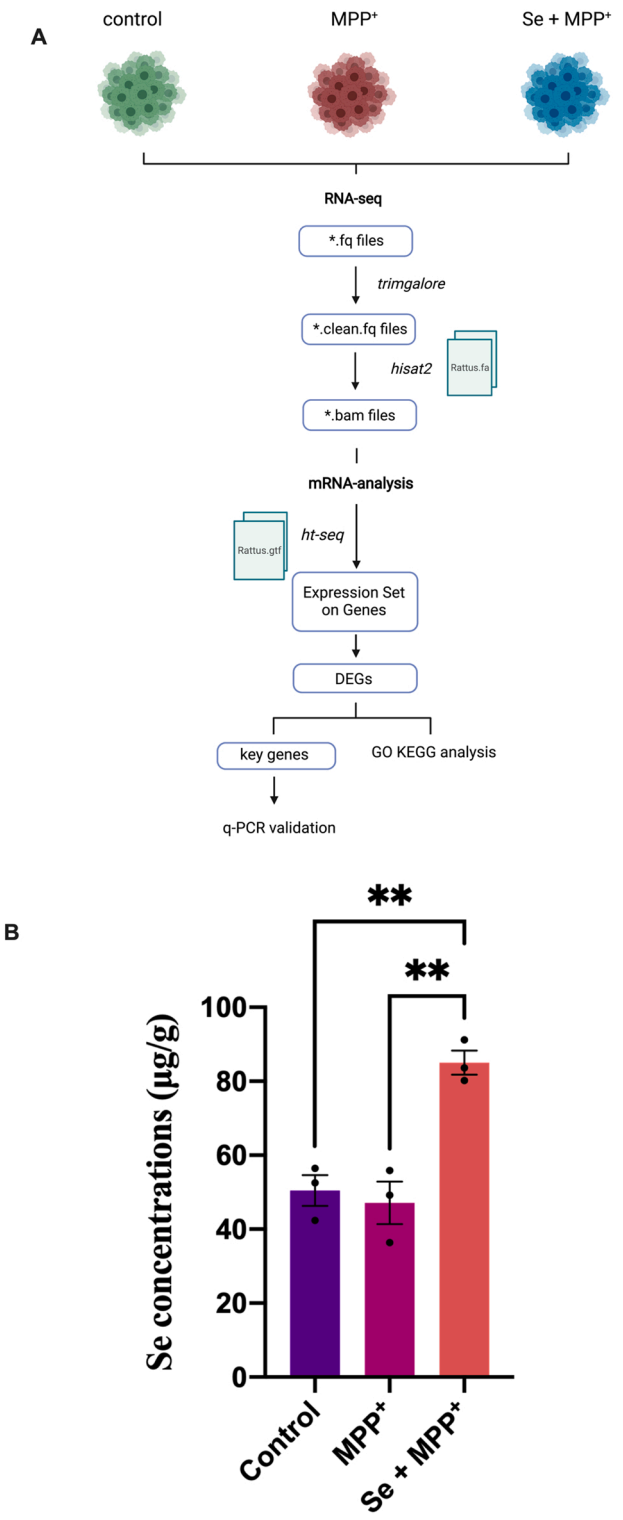

Fig. 2. (A) Flowchart of the study. Se can modulate MPP^+ induced cytotoxicity in PD cellular model. Total RNA, extracted from normal control group, MPP^+ group and Se + MPP^+ group, was sequenced to systematically investigate the protection mechanisms and pathways of Se. The methods and results are later described in detail. (B) Intracellular Se concentrations in the control group, MPP^+ group, and Se/MPP^+ group.

Comparison of sequencing data obtained from the MPP^+ group and control group showed that MPP^+ treatment altered gene expression in PC12 cells. Similarly, mRNAs and lncRNAs in the combination Se/MPP^+ group and MPP^+-only group showed gene expression in PC12 cells was altered by Se treatment. DEGs and DELs identified by comparing the MPP^+ group vs. the control group, as well as comparing the Se/MPP^+ group vs. MPP^+ group potentially identified DEGs and/or DELs that confer Se protective effects. We identified 351 DEGs in the MPP^+ group vs. control group, including 112 upregulated and 239 downregulated DEGs in the MPP^+ group (Supplementary Table 1). Heatmap and volcano plots (Fig. 3A and B, respectively) show gene expression patterns between the two groups. Comparing the combination Se/MPP^+ group with the MPP^+-only group, we also identified 244 DEGs, including 165 upregulated and 79 downregulated DEGs in Se/MPP^+ group (Fig. 3C, D and Supplementary Table 1). In group-wise comparisons of the MPP^+ group vs. control group, and Se/MPP^+ group vs. MPP^+-only group, 23 overlapping DEGs were identified. These DEG are considered as key DEGs that are potentially involved in regulating apoptosis and the level of reactive oxygen species (ROS) (Fig. 3E and Supplementary Table 2).

RNA sequencing also showed that 20 out of 24 total rodent selenoprotein genes were detected. Heatmap (Fig. 4A) analysis showing differential expression of selenoprotein genes in the control group, MPP^+ group, and Se/MPP^+ group indicated that most of these genes exhibit a higher expression level when compared to the Se-only treatment group. As shown in Fig. 4B, selenoprotein gene expression significantly increased when PC12 cells were exposed to Se. Among these selenoprotein genes, only thioredoxin reductase 1 (Txnrd1) has been shown to be a biomarker of Se exposure. The sequencing data further indicates no significant difference in selenoprotein gene expression between the MPP^+ group and the control group. However, when comparing the MPP^+ group and the Se/MPP^+ group, Txnrd1 had higher expression in the Se/MPP^+ group (Fig. 4A and Supplementary Table 1).

Compared with the control group, 14 DELs were observed in the MPP^+ group. Specifically, we found 10 upregulated and four downregulated DELs (Fig. 5A and B and Supplementary Table 1). Analysis of differential expression identified 27 DELs in the combination Se/MPP^+ group vs. MPP^+-only group, including 19 upregulated and eight downregulated lncRNAs (Fig. 5C and D and Supplementary Table 1).

3.3. GO terms and KEGG pathways analysis of DEGs reveal the protective Se function in MPP^+ induced PD model

To further determine the potential roles of DEGs in MPP^+ induced cytotoxicity and Se-associated protective effects, GO terms and KEGG pathway analysis was performed. The GO enriched terms of DEGs from the MPP^+ group vs. control group revealed DEGs involved in mitochondrial function, such as ATP synthesis coupled electron transport, glutathione metabolic processes, and mitochondrial respiratory chain complex III (Fig. 6A and Supplementary Table 3). In addition, a few identified terms were associated with protein heterodimerization and response to ROS. Using KEGG pathway analysis, DEGs from the MPP^+ group vs. control group were enriched in 39 pathways. Notably, some pathways were related to glutathione metabolism, p53 signaling, and oxidative phosphorylation (Fig. 6C and Supplementary Table 3). Of note, these terms appear relevant to mitochondrial dysfunction and protein aggregation associated with the pathogenesis of PD.

Analysis of the Se/MPP^+ group vs. MPP^+-only group, GO functional analysis results indicated antioxidant activity, cellular response to oxidative stress, and NADH metabolism (Fig. 6B and Supplementary Table 3). Moreover, some terms are related to protein catabolism, such as positive regulation of the proteasomal ubiquitin-dependent protein catabolism process and positive regulation of protein catabolism. Furthermore, in KEGG pathway analysis, DEGs were identified that annotated to 49 pathways, some of which were associated with

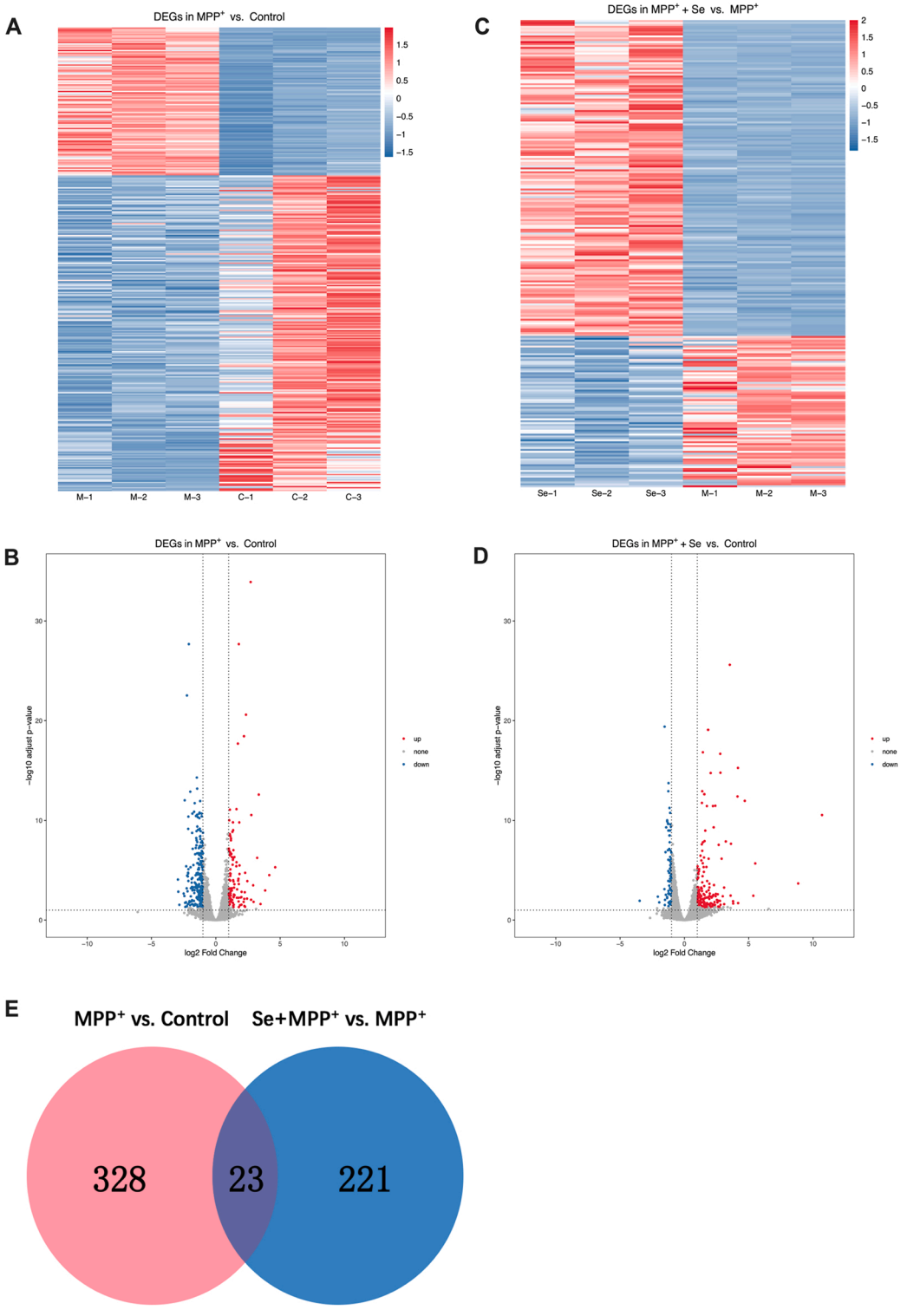

Fig. 3. Identification of DEGs. (A) Heatmap showing differential expressions of DEGs from MPP^+ group vs. normal control group. (B) Volcano plots showing the upregulated and downregulated genes in MPP^+ group vs. normal control group. (C) Heatmap showing differential expressions of DEGs from MPP^+ group vs. Se/MPP^+ group. (D) Volcano plots showing the upregulated and downregulated genes in MPP^+ group vs. Se/MPP^+ group. (E) Venn showing analysis of unique and shared DEGs between MPP^+ group vs. normal control group and MPP^+ group vs. Se/MPP^+ group.

mitochondrial control of apoptosis, such as PI3K-Akt signaling pathway, TNF signaling pathway, and NF-kappa B signaling pathway (Fig. 6C and Supplementary Table 3). Altogether, these terms may indicate how Se protects against mitochondrial dysfunction and apoptosis.

3.4. Validation of sequencing data using RT-qPCR

To verify our sequencing results, we randomly selected five DEGs (Col6a3, Gadd45b, Klf2, Pdk4 and Gpr37) from the list of key DEGs that were obtained by comparing both MPP^+ group vs. control group, and Se/MPP^+ group vs. MPP^+-only group. The expression of these DEGs were subsequently validated using RT-qPCR. RT-qPCR results from an independently prepared set of cells showed the expression of Col6a3 was upregulated in the MPP^+ group, while Gadd45b, Klf2, Pdk4 and Gpr37 were downregulated. Gadd45b, Klf2 and Pdk4 were upregulated, and Col6a3 and Gpr37 were downregulated in Se/MPP^+ group vs. the MPP^+-only group. This RT-qPCR analysis is consistent with the data obtained from RNA sequencing (Fig. 7).

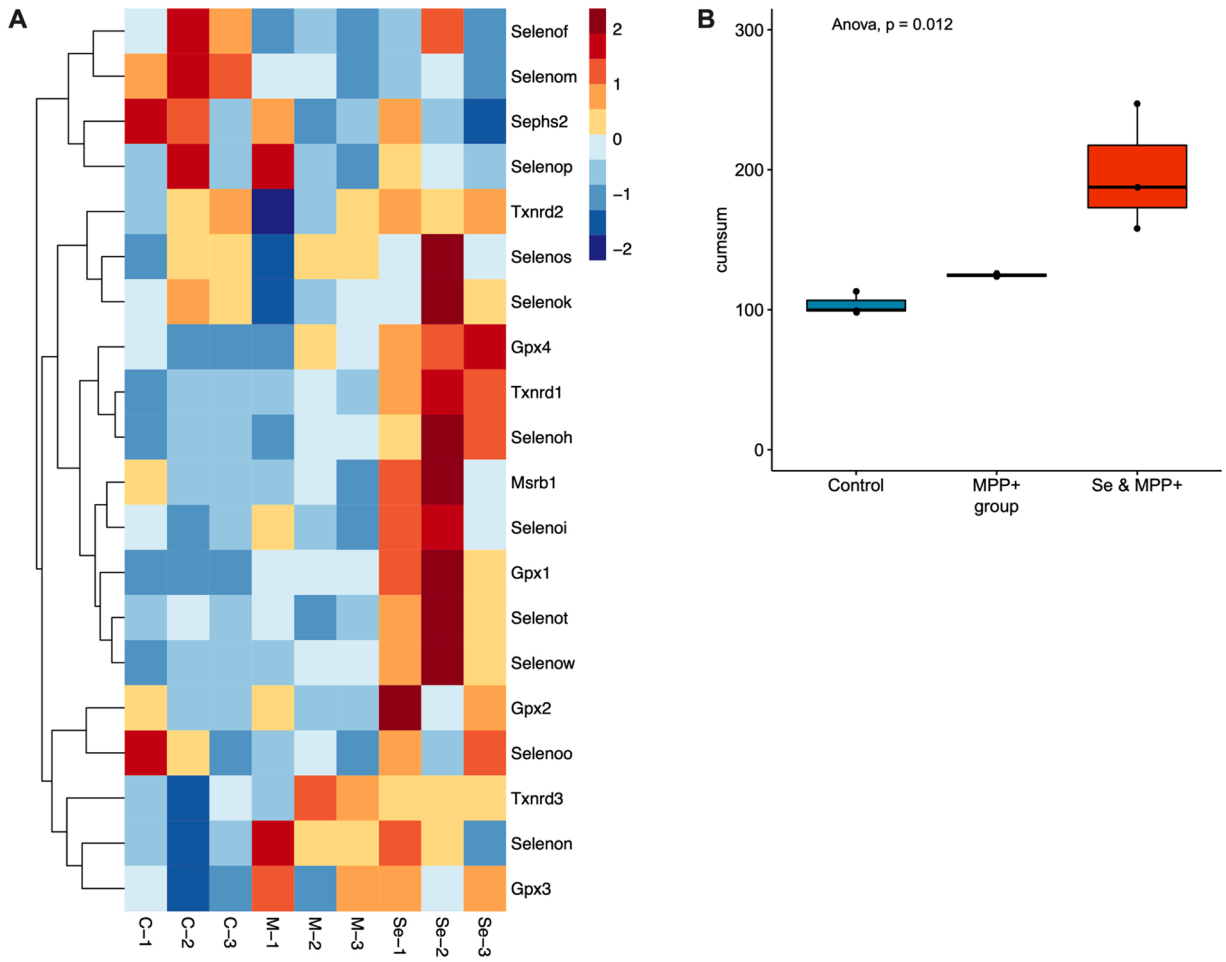

Fig. 4. Selenoprotein transcript expression. (A) Heatmap showing differential expressions of selenoprotein genes in the control group, MPP^+ group and Se/MPP^+ group. (B) The comparison of accumulative selenoprotein genes expression among the control group, MPP^+ group and Se/MPP^+ group.

3.5. Supplement of MPP^+ or/and Se lead to DELs and functional analysis of cis-targeted genes

A substantial fraction of lncRNAs, namely *cis*-acting lncRNAs, modulate the expression of coding genes, in a way dependent varying distances from target genes to the location of the site of their transcription [28]. As many mechanisms of action have been documented, *cis*-acting lncRNAs could activate, repress, or otherwise regulate gene expression. To further investigate the potential function of lncRNAs in response to MPP^+ or/and Se treatment, *cis*-target gene functions were annotated using GO and KEGG pathway enrichment analysis. In the MPP^+ group vs. control group, the results indicated 14 DELs corresponding to 57 *cis*-target genes (Fig. 8A and Supplementary Table 4). The lncRNA *cis*-target genes were related by GO terms, including glutathione biosynthetic process, cell aging, and negative regulation of the ATP metabolic process. Further, KEGG pathways, including taurine and hypotaurine metabolism, and spliceosome function (Fig. 9A and C, Supplementary Table 3) were identified. In addition, these analyses identified 70 predicted *cis*-target genes in the Se/MPP^+ group vs. MPP^+-only group (Fig. 8B and Supplementary Table 4). GO enrichment analysis showed that these *cis*-target genes were enriched in genes linked to modulation of age-related behavioral decline, intrinsic apoptotic signaling pathway in response to DNA damage by p53 class mediator, and cellular response to hydrogen peroxide. Using KEGG pathway analysis, terms associated to lysosome function, PI3K-Akt signaling, and the Wnt signaling pathway (Fig. 9B and C, Supplementary Table 3) were observed. These terms indicate that Se could resist MPP^+ induced neuron death by limiting apoptosis.

4. Discussion

PD represents a common and complex neurological disorder, the pathogenesis of which is largely unknown. Overwhelming evidence suggests that mitochondrial dysfunction plays an important role in PD pathophysiology [29]. Se, considered a cornerstone antioxidant, can augment the adverse effects of mitochondrial dysfunction [30] and previous studies indicate a protective effect of Se in PD [11–13]. However, to date, the mechanisms and pathways associated with regulating the protective effect of Se in PD have not been systematically studied. In this study, Se was shown to reverse the loss of PC12 viability in a MPP^+-induced cellular model of PD. We subsequently performed high-throughput sequencing to identify DEGs and DELs, and explored the possible mechanisms and pathways involved in the protective function of Se.

MPP^+ impairs mitochondrial function and leads to ROS-associated insult in a PD model [22]. These conclusions agree with our GO analysis of DEGs from MPP^+ group vs. normal control group, which are associated with ATP synthesis-coupled electron transport, response to ROS, as well as KEGG pathway analysis which showed links to oxidative phosphorylation and glutathione metabolism. Furthermore, some identified terms involved in protein heterodimerization activity were observed. Of note, protein dimerization has been linked to the pathogenesis of PD [31,32] such as alpha-synuclein aggregation in a continuous low-level MPTP-induced PD model [33]. In the combination

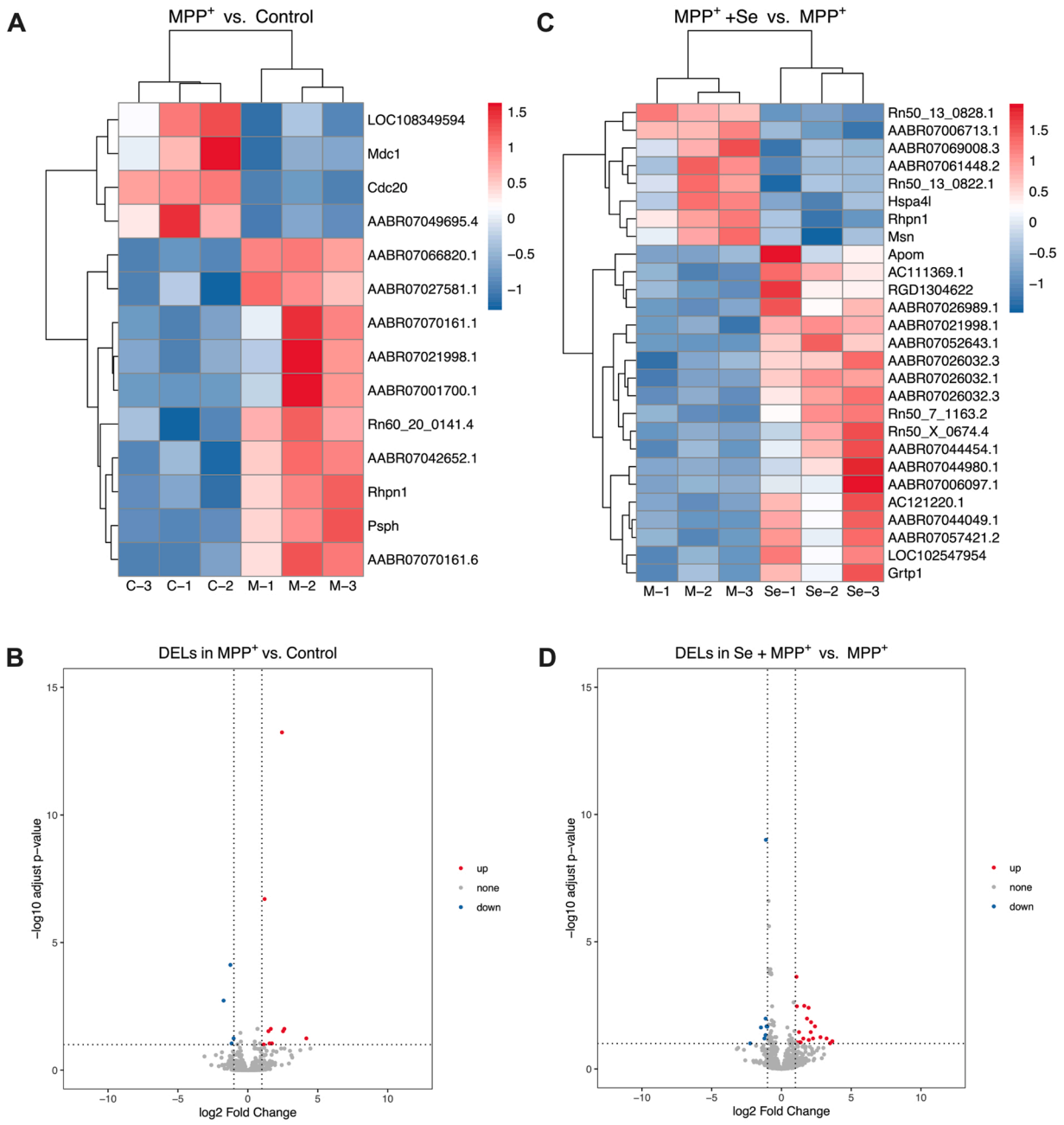

Fig. 5. Identification of DELs. (A) Heatmap showing differential expressions of DELs from MPP^+ group vs. normal control group. (B) Volcano plots showing the upregulated and downregulated lncRNAs in MPP^+ group vs. normal control group. (C) Heatmap showing differential expressions of DELs from MPP^+ group vs. Se/MPP^+ group. (D) Volcano plots showing the upregulated and downregulated lncRNAs in MPP^+ group vs. Se/MPP^+ group.

Se/MPP^+ group vs. the MPP^+-only group, GO analysis of DEGs implies that Se has the potential to reduce the damage of reactive species and enhance detoxification. As suggested by our KEGG pathway analysis, Se protective function may involve resisting mitochondrial control of apoptosis through p53 and/or TNF signaling [34,35].

The mechanism(s) underlying the Se-dependent regulation of selenoprotein transcript levels is not understood. For GPx1 and GPx4 mRNA this regulation appears to not be due to transcriptional regulation nor attributable to mRNA processing and export from the nucleus [36,37]. It had been reported that in different cell lines that varying Se concentrations and treatment times can lead to differential expression of selenoprotein genes. In heat stress models, Se supplementation (0.5 μM) increased the expression of 5 selenoprotein genes (GPx1, glutathione peroxidase 3 (GPx3), selenoprotein H (Selenoh), Selenos, and selenoprotein W (Selenow). In contrast, Se decreased 3 genes, namely, selenoprotein O (Selenoo), selenophosphate synthetase 2 (Sephs2), and thioredoxin reductase 3 (Txnrd3). Moreover, different treatment times also led to differences in selenoprotein gene expression [38]. The addition of 10 μM Se to cultures of the mouse epithelial line F-9 led to an increase in the mRNA levels of GPX1, 2, and 4, and a substantial reduction in the expression level of Txnrd1 and Txnrd [39]. In this study, when PC12 cells were treated with 20 μM Se for 36 h, the intracellular Se concentrations became higher and the total selenoprotein gene expression significant increased. In addition, only Txnrd1 was differentially expressed among all the 24 rodent selenoprotein genes. Txnrd1 may be a biomarker for Se status in our PD cellular model, and may play an important role in the protective function of Se in PD. Knocking out Txnrd1 in the mouse nervous system led to ataxia and tremor, and

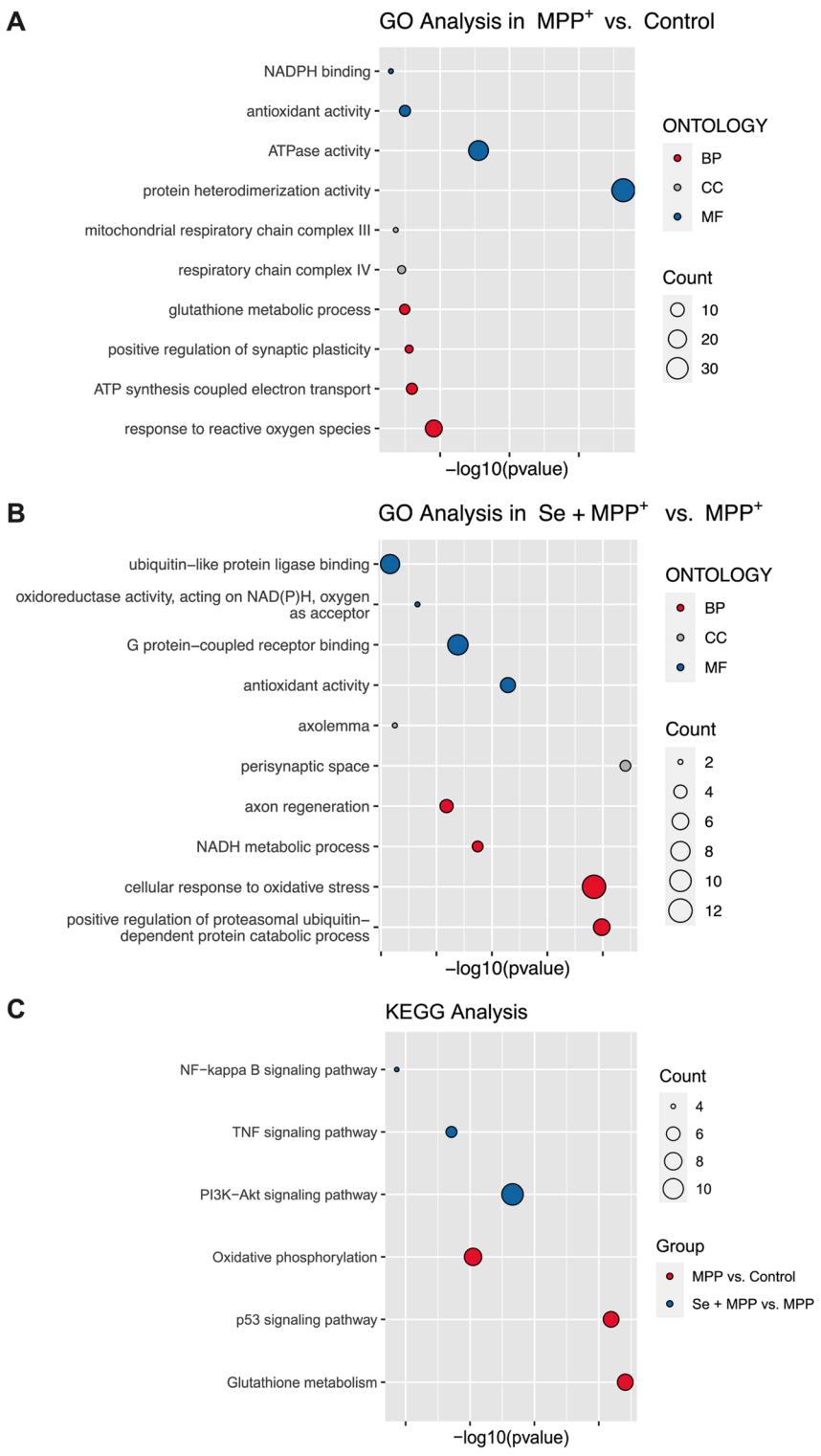

Fig. 6. Functional enrichment analysis of DEGs. (A) GO analysis for DEGs in MPP^+ group vs. normal control group. (B) GO analysis for DEGs in MPP^+ group vs. Se/MPP^+ group. (C) KEGG enrichment pathways for DEGs in MPP^+ group vs. normal control group and in MPP^+ group vs. Se/MPP^+ group.

highlighted the association between Txnrd1 and PD [40]. Some studies showed that Txnrd1 could reduce DNA damage, mitochondrial autophagy, and ER stress by abrogating cell death through the GSK-3β/NF-κB signaling pathway in a PD model [41–43]. These findings have led to the view that overexpression of Txnrd1 has a protective function in PD.

In terms of GO analysis, Txnrd1 was found to be associated with cellular detoxification. Txnrd1 is involved in the thioredoxin pathway, which is a significant reductive system in mammalian cells [44]. This system plays a key role in protecting cells from oxidative stress and apoptosis [42,45], thus indicating that Txnrd1 can modulate MPP^+-induced cytotoxicity. More importantly, Txnrd1 is involved in ROS and NADP metabolism. Nagakannan et al. reported that enhanced oxidative stress inhibited the ubiquitination-proteasome system and impaired the final stages of autophagy by inhibiting lysosomal activity [46]. Thus, these results suggest that Txnrd1 could regulate degradation of abnormal aggregation of proteins and lysosomal-associated autophagy

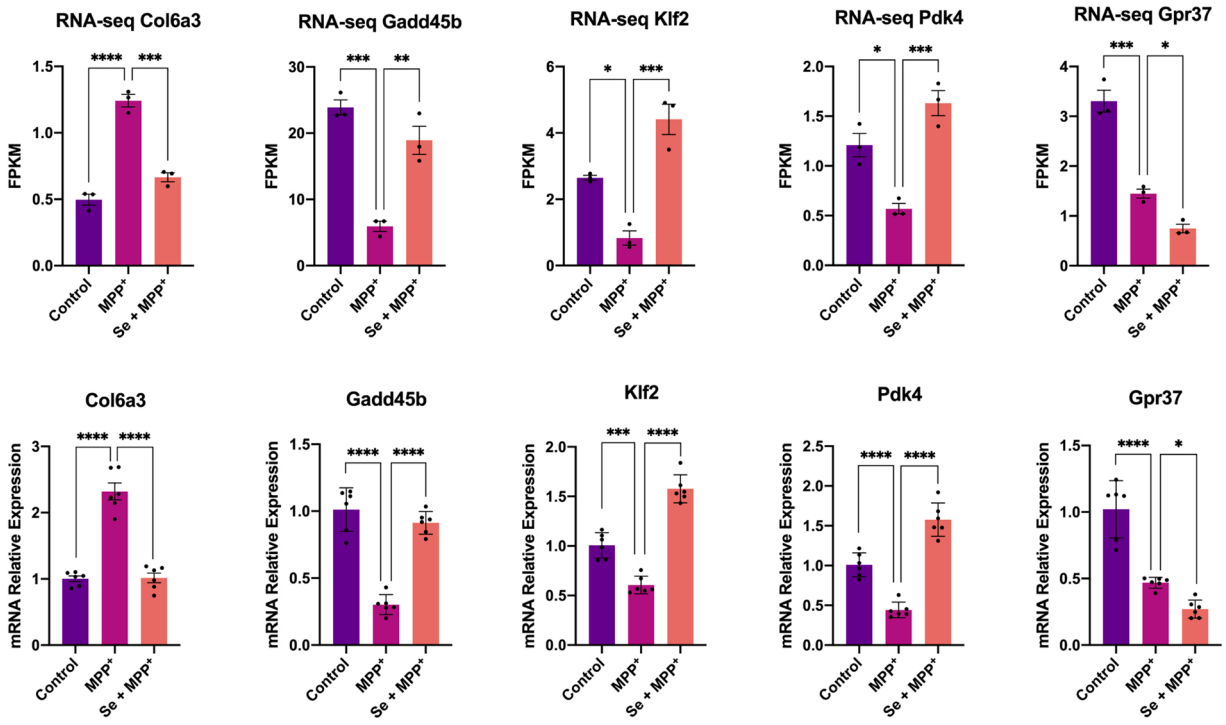

Fig. 7. Validation of RNA-sequencing data by RT-qPCR. Eight randomly selected DEGs from normal control group, MPP^+ group and Se/MPP^+ group are presented as relative gene expression (n = 6). Error bars indicate mean ± SEM (n = 6). *p < 0.05, * *p < 0.01, * **p < 0.001 and * ** *p < 0.0001.

to postpone progression of PD [2]. In our in vitro study, Se treatment could upregulate the expression of Txnrd1. Therefore, Se and Txnrd1 may represent a novel neuroprotective strategy for PD.

Using RNA sequencing, 23 DEGs were found to overlap between the MPP^+ group vs. control group, and combination Se/MPP^+ group vs. MPP^+-only group. These DEGs we deem to be the key genes involved in Se protective function. The key DEG sialoadhesin (Siglec1) is a macrophage-restricted glycoprotein that promotes neuroinflammation [47,48]. In multiple sclerosis, pathogenic phagocytosis enhances the expression of Siglec1 and contributes to neuroinflammation [49]. The expression of Siglec1 was induced by MPP^+ and suppressed by Se in our study (Supplementary Table 1). Thus, this result suggests that Se may protect cells from neuroinflammation and pathogenic phagocytosis by attenuating Siglec1 expression.

Another key DEG, krueppel-like factor 2 (Klf2), is a zinc finger transcription factor that appears to respond to ROS [50]. Using GO analysis, Klf2 was found to be particularly associated with oxidative stress. In Alzheimer's disease, overexpression of Klf2 could alleviate oxidative stress and attenuate apoptosis [51]. Our RNA sequencing data revealed that the expression of Klf2 was downregulated in the MPP^+-only group and upregulated in the Se/MPP^+ group (Supplementary Table 1), which suggested that Se has anti-apoptotic and cytoprotective roles in vitro. Moreover, Klf2 can regulate mitophagy and mitochondrial metabolism [52]. Mitophagy helps maintain cellular and mitochondrial homeostasis by clearing impaired mitochondria [53], and our findings suggest that Se may also reduce mitochondrial dysfunction by inducing Klf2 expression in our PD cellular model.

This study also analyzed several DELs. To better understand the role of DELs in Se protective functions in PD, a lncRNA–mRNA network was established (Fig. 8A and B). Per KEGG pathway analysis of DELs from the Se/MPP^+ group vs. the MPP^+-only group, some terms were associated with PI3K-Akt and FoxO signaling pathway. These terms are related to a potential target gene, specifically, Cyclin-dependent kinase inhibitor 1 (Cdkn1a). Cdkn1a, a *cis*-element of AABR07044454.1, was identified as a potent inhibitor of cell cycle progression [54]. Our sequencing data reveals that the expression of Cdkn1a and AABR07044454.1 were increased in Se + MPP^+ group (Supplementary Table 1). In PD pathogenesis, leucine-rich repeat kinase 2 which has been implicated as a PD-causative gene, was found to phosphorylate p53. This event, in turn, induces Cdkn1a expression and apoptosis in differentiated SH-SY5Y cells and rat primary neurons [55]. However, this does not mean that Cdkn1a, when induced by leucine-rich repeat kinase 2, leads to apoptosis. Suzuki et al. reported that a procaspase 3/Cdkn1a complex could resist Fas-mediated apoptosis in HepG2 cells [56]. Cadkn1a is associated with inflammation as a $Cdkn1a^{-/-}$ mouse model showed enhanced inflammation during osteoarthritis [57]. Altogether, these results suggest that AABR07044454.1, when induced by Se, might activate Cdkn1a expression and protect PC12 cells from MPP^+-induced apoptosis and block inflammation.

In this work, several genes such as Txnrd1, Siglec1, and Klf2, as well as lncRNA AABR07044454.1 working in *cis* on the target gene Cdkn1a may have a protective function in PD. However, a limitation of this study is that we do not provide experimental proof to confirm the underlying mechanism and infer functional connections between lncRNA and target genes. Furthermore, all the results were from an experimental in vitro model. Future studies will require the study of these potential mechanisms and pathways to better understand the protective function of Se in vivo.

5. Conclusions

We have found that Se modulates MPP^+ insult in an in vitro PD model. The gene expression profiles of a control group, MPP^+-only group and combination Se/MPP^+ group were revealed by transcriptomic analysis. Among these three transcriptomes analyzed, some DEGs and DELs were identified, and these may contribute to the cytoprotective function of Se in PD. By combining the data sets of DEGs and DELs from different treatment groups, these DEGs and DELs may play a part in PD, such as protecting against oxidative stress and neuroinflammation, and prevent dopamine neurons from damage and apoptosis. The results of our study provide novel information into the cytoprotective mechanisms of Se in a cellular PD model, and identify

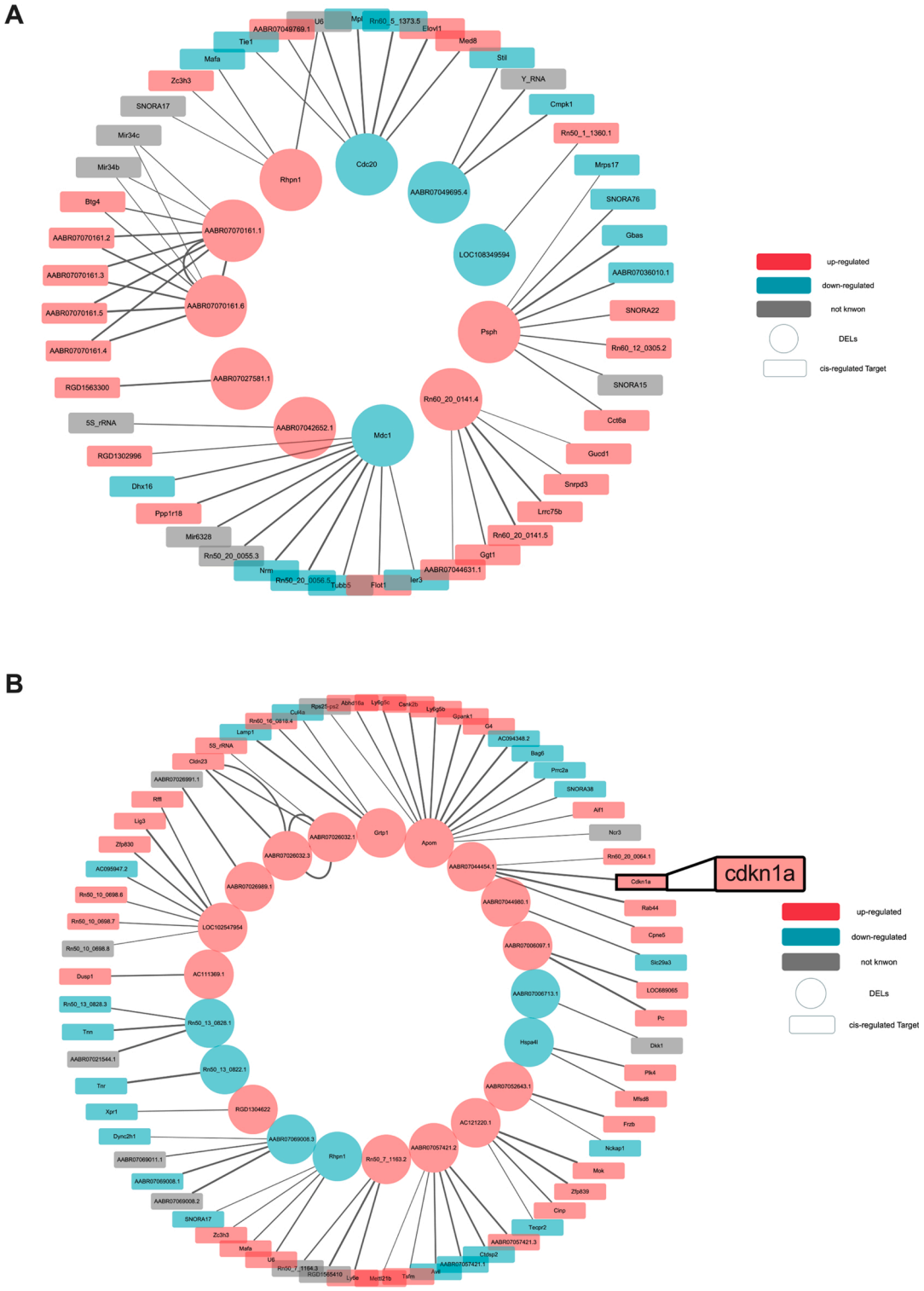

Fig. 8. LncRNA–mRNA networks. (A) In MPP^+ group vs. normal control group comparison, 14 DELs are cis-acting with 57 mRNAs, which build the interactive network. (B) In MPP^+ group vs. Se/MPP^+ group comparison, 27 DELs are cis-acting with 70 mRNAs, which build the interactive network. The thickness of the lines represents the distance from target genes to the location of their own transcription sites and the thinner the line, the farther away from transcription sites.

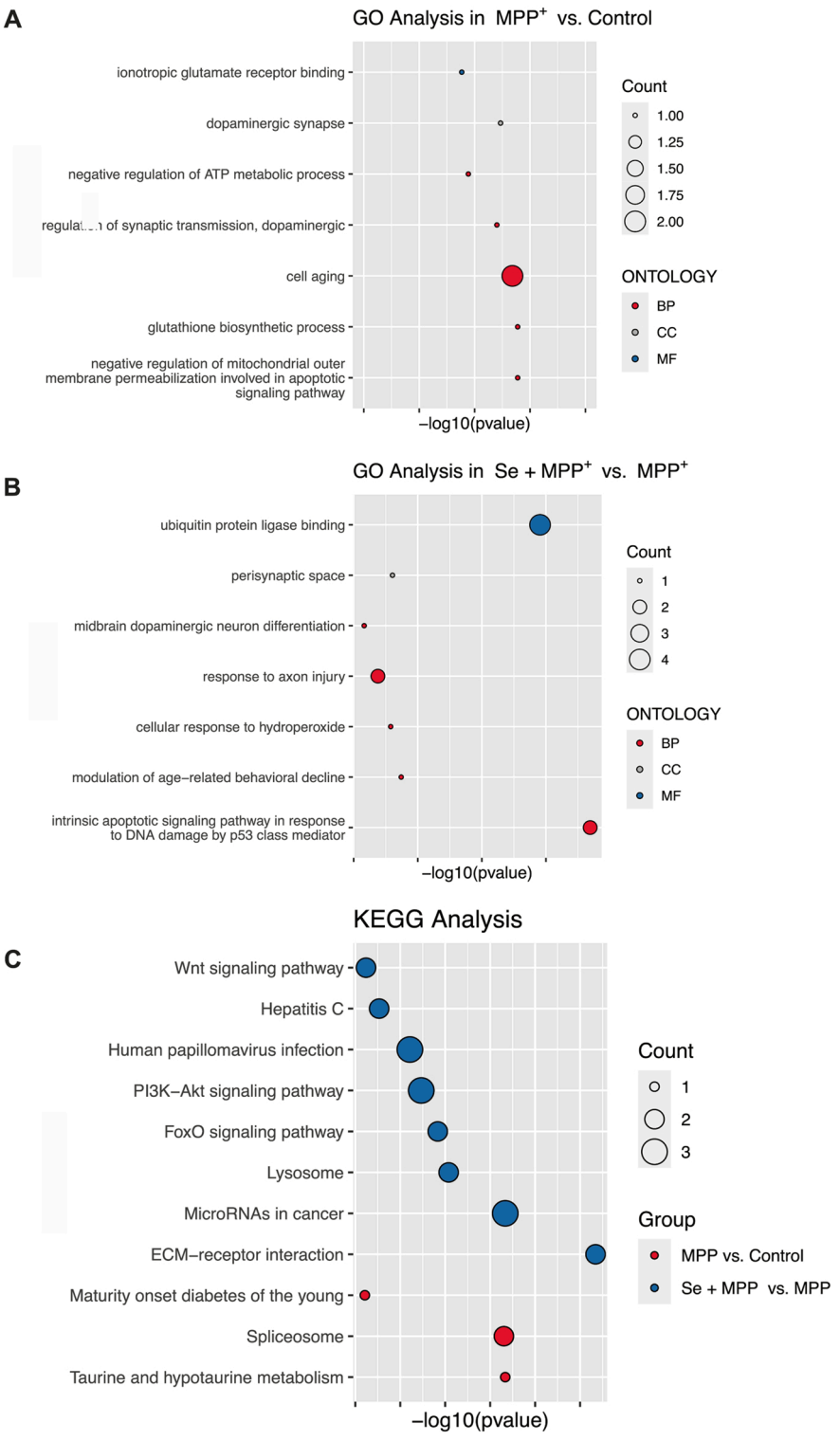

Fig. 9. Functional enrichment analysis of DELs. (A) GO analysis for potential target genes of DELs in MPP^+ group vs. normal control group. (B) GO analysis for potential target genes of DELs in MPP^+ group vs. Se/MPP^+ group. (C) KEGG enrichment pathways for potential target genes of DELs in MPP^+ group vs. normal control group and in MPP^+ group vs. Se/MPP^+ group.

potential candidate lncRNAs and genes related to the prevention and treatment of PD.

Funding

This study was financially supported by the Geological Survey Project of China Geological Survey (Granted No. DD20211414).

CRediT authorship contribution statement

Conceptualization, **Wei Wei**, **Rui Gong** and **Jincao Chen**; Methodology, **Wen Liu** and **Xiang Li**; validation, **Wei Wei** and **Xiang Li**; Resources, **Wu Liang**, **Chenguang Jia** and **Jie Zhang**; Data curation, **Feiyang Zhang**; Writing – original draft preparation, **Wen Liu**, **Feiyang Zhang** and **Wu Liang**; Writing – review and editing, **Wei Wei**, **Xiang Li**

and **Jincao Chen**; Visualization, **Feiyang Zhang** and **Kaixin Huang**; Supervision, **Rui Gong** and **Jincao Chen**. All authors have read and agreed to the published version of the manuscript.

Declaration of Competing Interest

We wish to confirm that there are no known conflicts of interest associated with this publication and there has been no significant financial support for this work that could have influenced its outcome.

Appendix A. Supporting information

Supplementary data associated with this article can be found in the online version at doi:10.1016/j.jtemb.2023.127208.

References

[1] B.R. Bloem, M.S. Okun, C. Klein, Parkinson's disease, Lancet 397 (10291) (2021) 2284–2303.
[2] A.H. Schapira, P. Jenner, Etiology and pathogenesis of Parkinson's disease, Mov. Disord. 26 (6) (2011) 1049–1055.
[3] M.J. Armstrong, M.S. Okun, Diagnosis and treatment of parkinson disease: a review, JAMA 323 (6) (2020) 548–560.
[4] M.P. Rayman, Selenium and human health, Lancet 379 (9822) (2012) 1256–1268.
[5] O.M. Guillin, C. Vindry, T. Ohlmann, L. Chavatte, Selenium, selenoproteins and viral infection, Nutrients 11 (9) (2019).
[6] M.A. Reeves, P.R. Hoffmann, The human selenoproteome: recent insights into functions and regulation, Cell Mol. Life Sci. 66 (15) (2009) 2457–2478.
[7] Z.H. Zhang, G.L. Song, Roles of selenoproteins in brain function and the potential mechanism of selenium in Alzheimer's disease, Front. Neurosci. 15 (2021).
[8] J.H. Ellwanger, S.I. Franke, D.L. Bordin, D. Pra, J.A. Henriques, Biological functions of selenium and its potential influence on Parkinson's disease, Acad. Bras. Cienc. 88 (3 Suppl) (2016) 1655–1674.
[9] B.R. Cardoso, B.R. Roberts, A.I. Bush, D.J. Hare, Selenium, selenoproteins and neurodegenerative diseases, Metallomics 7 (8) (2015) 1213–1228.
[10] X. Zhang, R.P. Liu, W.H. Cheng, J.H. Zhu, Prioritized brain selenium retention and selenoprotein expression: nutritional insights into Parkinson's disease, Mech. Ageing Dev. 180 (2019) 89–96.
[11] J.H. Ellwanger, P. Molz, D.R. Dallemole, A. Pereira dos Santos, T.E. Muller, L. Cappelletti, M. Goncalves da Silva, S.I. Franke, D. Pra, J.A. Pegas Henriques, Selenium reduces bradykinesia and DNA damage in a rat model of Parkinson's disease, Nutrition 31 (2) (2015) 359–365.
[12] H. Kim, W. Jhoo, E. Shin, G. Bing, Selenium deficiency potentiates methamphetamine-induced nigral neuronal loss; comparison with MPTP model, Brain Res 862 (1–2) (2000) 247–252.
[13] H.A. Khan, Selenium partially reverses the depletion of striatal dopamine and its metabolites in MPTP-treated C57BL mice, Neurochem Int 57 (5) (2010) 489–491.
[14] L. Boukhzar, A. Hamieh, D. Cartier, Y. Tanguy, I. Alsharif, M. Castex, A. Arabo, S. El Hajji, J.J. Bonnet, M. Errami, A. Falluel-Morel, A. Chagraoui, I. Lihrmann, Y. Anouar, Selenoprotein T exerts an essential oxidoreductase activity that protects dopaminergic neurons in mouse models of Parkinson's disease, Antioxid. Redox Signal 24 (11) (2016) 557–574.
[15] F.P. Bellinger, A.V. Raman, R.H. Rueli, M.T. Bellinger, A.S. Dewing, L.A. Seale, M. A. Andres, J.H. Uyehara-Lock, L.R. White, G.W. Ross, M.J. Berry, Changes in selenoprotein P in substantia nigra and putamen in Parkinson's disease, J. Park. Dis. 2 (2) (2012) 115–126.
[16] I. Ingold, C. Berndt, S. Schmitt, S. Doll, G. Poschmann, K. Buday, A. Roveri, X. Peng, F. Porto Freitas, T. Seibt, L. Mehr, M. Aichler, A. Walch, D. Lamp, M. Jastroch, S. Miyamoto, W. Wurst, F. Ursini, E.S.J. Arnér, N. Fradejas-Villar, U. Schweizer, H. Zischka, J.P. Friedmann Angeli, M. Conrad, Selenium Utilization by GPX4 Is Required to Prevent Hydroperoxide-Induced Ferroptosis, Cell 172 (3) (2018) 409–422, e21.
[17] A.M. Raines, R.A. Sunde, Selenium toxicity but not deficient or super-nutritional selenium status vastly alters the transcriptome in rodents, BMC Genom. 12 (2011) 26.
[18] H. Hugejiletu, G. Bobe, W.R. Vorachek, M.E. Gorman, W.D. Mosher, G.J. Pirelli, J. A. Hall, Selenium supplementation alters gene expression profiles associated with innate immunity in whole-blood neutrophils of sheep, Biol. Trace Elem. Res 154 (1) (2013) 28–44.
[19] J. Yang, Y. Gong, J. Cai, Q. Liu, Z. Zhang, lnc-3215 suppression leads to calcium overload in selenium deficiency-induced chicken heart lesion via the lnc-3215-miR-1594-TNN2 pathway, Mol. Ther. Nucleic Acids 18 (2019) 1–15.
[20] Z.Z. Liang, R.M. Zhu, Y.L. Li, H.M. Jiang, R.B. Li, Q. Wang, L.Y. Tang, Z.F. Ren, Differential epigenetic profiles induced by sodium selenite in breast cancer cells, J. Trace Elem. Med Biol. 64 (2021), 126677.
[21] A. Dominiak, A. Wilkaniec, H. Jęśko, G.A. Czapski, A.M. Lenkiewicz, E. Kurek, P. Wroczyński, A. Adamczyk, Selol, an organic selenium donor, prevents lipopolysaccharide-induced oxidative stress and inflammatory reaction in the rat brain, Neurochem Int 108 (2017) 66–77.
[22] B.H. Falkenburger, T. Saridaki, E. Dinter, Cellular models for Parkinson's disease, J. Neurochem 139 (Suppl 1) (2016) 121–130.
[23] S.H. Snyder, R.J. D'Amato, MPTP: a neurotoxin relevant to the pathophysiology of Parkinson's disease. The 1985 George C. Cotzias lecture, Neurology 36 (2) (1986) 250–258.
[24] M. Rostamian Delavar, M. Baghi, Z. Safaeinejad, A. Kiani-Esfahani, K. Ghaedi, M. H. Nasr-Esfahani, Differential expression of miR-34a, miR-141, and miR-9 in MPP +-treated differentiated PC12 cells as a model of Parkinson's disease, Gene 662 (2018) 54–65.
[25] M. Ashburner, C.A. Ball, J.A. Blake, D. Botstein, H. Butler, J.M. Cherry, A.P. Davis, K. Dolinski, S.S. Dwight, J.T. Eppig, M.A. Harris, D.P. Hill, L. Issel-Tarver, A. Kasarskis, S. Lewis, J.C. Matese, J.E. Richardson, M. Ringwald, G.M. Rubin, G. Sherlock, Gene ontology: tool for the unification of biology. The Gene Ontology Consortium, Nat. Genet 25 (1) (2000) 25–29.
[26] M. Kanehisa, S. Goto, KEGG: kyoto encyclopedia of genes and genomes, Nucleic Acids Res 28 (1) (2000) 27–30.
[27] M. Ran, B. Chen, Z. Li, M. Wu, X. Liu, C. He, S. Zhang, Z. Li, Systematic identification of long noncoding RNAs in immature and mature porcine testes, Biol. Reprod. 94 (4) (2016) 77.
[28] N. Gil, I. Ulitsky, Regulation of gene expression by cis-acting long non-coding RNAs, Nat. Rev. Genet 21 (2) (2020) 102–117.
[29] J.S. Park, R.L. Davis, C.M. Sue, Mitochondrial dysfunction in parkinson's disease: new mechanistic insights and therapeutic perspectives, Curr. Neurol. Neurosci. Rep. 18 (5) (2018) 21.
[30] O.L. Adebayo, G.A. Adenuga, R. Sandhir, Selenium and zinc protect brain mitochondrial antioxidants and electron transport chain enzymes following postnatal protein malnutrition, Life Sci. 152 (2016) 145–155.
[31] A.T. Medeiros, L.G. Soll, I. Tessari, L. Bubacco, J.R. Morgan, alpha-synuclein dimers impair vesicle fission during clathrin-mediated synaptic vesicle recycling, Front Cell Neurosci. 11 (2017) 388.
[32] M. Nguyen, Y.C. Wong, D. Ysselstein, A. Severino, D. Krainc, Synaptic, mitochondrial, and lysosomal dysfunction in Parkinson's disease, Trends Neurosci. 42 (2) (2019) 140–149.
[33] F. Fornai, O.M. Schluter, P. Lenzi, M. Gesi, R. Ruffoli, M. Ferrucci, G. Lazzeri, C. L. Busceti, F. Pontarelli, G. Battaglia, A. Pellegrini, F. Nicoletti, S. Ruggieri, A. Paparelli, T.C. Sudhof, Parkinson-like syndrome induced by continuous MPTP infusion: convergent roles of the ubiquitin-proteasome system and alpha-synuclein, Proc. Natl. Acad. Sci. USA 102 (9) (2005) 3413–3418.
[34] C. Perier, J. Bové, D.C. Wu, B. Dehay, D.K. Choi, V. Jackson-Lewis, S. Rathke-Hartlieb, P. Bouillet, A. Strasser, J.B. Schulz, S. Przedborski, M. Vila, Two molecular pathways initiate mitochondria-dependent dopaminergic neurodegeneration in experimental Parkinson's disease, Proc. Natl. Acad. Sci. USA 104 (19) (2007) 8161–8166.
[35] B. Ferger, A. Leng, A. Mura, B. Hengerer, J. Feldon, Genetic ablation of tumor necrosis factor-alpha (TNF-alpha) and pharmacological inhibition of TNF-synthesis attenuates MPTP toxicity in mouse striatum, J. Neurochem 89 (4) (2004) 822–833.
[36] M.J. Christensen, K.W. Burgener, Dietary selenium stabilizes glutathione peroxidase mRNA in rat liver, J. Nutr. 122 (8) (1992) 1620–1626.
[37] H. Toyoda, S. Himeno, N. Imura, Regulation of glutathione peroxidase mRNA level by dietary selenium manipulation, Biochim Biophys. Acta 1049 (2) (1990) 213–215.
[38] Y. Liu, A. He, J. Tang, A.M. Shah, G. Jia, G. Liu, G. Tian, X. Chen, J. Cai, B. Kang, H. Zhao, Selenium alleviates the negative effect of heat stress on myogenic differentiation of C2C12 cells with the response of selenogenome, J. Therm. Biol. 97 (2021), 102874.
[39] Y.P. Kuznetsova, M.V. Goltyaev, O.S. Gorbacheva, S.V. Novoselov, E.G. Varlamova, E.E. Fesenko, Influence of sodium selenite on the mRNA expression of the mammalian selenocysteine-containing protein genes in testicle and prostate cancer cells, Dokl. Biochem Biophys. 480 (1) (2018) 131–134.
[40] J. Soerensen, C. Jakupoglu, H. Beck, H. Förster, J. Schmidt, W. Schmahl, U. Schweizer, M. Conrad, M. Brielmeier, The role of thioredoxin reductases in brain development, PLoS One 3 (3) (2008), e1813.
[41] Z. Liu, Q. Ye, F. Wang, Y. Guo, R. Cui, J. Wang, D. Wang, Protective effect of thioredoxin reductase 1 in Parkinson's disease, Neurosci. Lett. 741 (2021), 135457.
[42] Z. Liu, Q. Ye, F. Wang, Y. Guo, R. Cui, J. Wang, D. Wang, Overexpression of thioredoxin reductase 1 can reduce DNA damage, mitochondrial autophagy and endoplasmic reticulum stress in Parkinson's disease, Exp. Brain Res. 239 (2) (2021) 475–490.
[43] L. Arodin, A. Miranda-Vizuete, P. Swoboda, A.P. Fernandes, Protective effects of the thioredoxin and glutaredoxin systems in dopamine-induced cell death, Free Radic. Biol. Med 73 (2014) 328–336.
[44] M. Dagnell, E.E. Schmidt, E.S.J. Arnér, The A to Z of modulated cell patterning by mammalian thioredoxin reductases, Free Radic. Biol. Med 115 (2018) 484–496.
[45] R. Pillai, J.H. Uyehara-Lock, F.P. Bellinger, Selenium and selenoprotein function in brain disorders, IUBMB Life 66 (4) (2014) 229–239.
[46] P. Nagakannan, M.A. Iqbal, A. Yeung, J.A. Thliveris, M. Rastegar, S. Ghavami, E. Eftekharpour, Perturbation of redox balance after thioredoxin reductase deficiency interrupts autophagy-lysosomal degradation pathway and enhances cell death in nutritionally stressed SH-SY5Y cells, Free Radic. Biol. Med 101 (2016) 53–70.
[47] S.S. Siddiqui, R. Matar, M. Merheb, R. Hodeify, C.G. Vazhappilly, J. Marton, S. A. Shamsuddin, H. Al Zouabi, Siglecs in brain function and neurological disorders, Cells 8 (10) (2019).
[48] J. Groh, E. Ribechini, D. Stadler, T. Schilling, M.B. Lutz, R. Martini, Sialoadhesin promotes neuroinflammation-related disease progression in two mouse models of CLN disease, Glia 64 (5) (2016) 792–809.

[49] J.F. Bogie, E. Boelen, E. Louagie, P. Delputte, D. Elewaut, J. van Horssen, J. J. Hendriks, N. Hellings, CD169 is a marker for highly pathogenic phagocytes in multiple sclerosis, Mult. Scler. 24 (3) (2018) 290–300.
[50] X. Gao, S. Jiang, Z. Du, A. Ke, Q. Liang, X. Li, KLF2 protects against osteoarthritis by repressing oxidative response through activation of Nrf2/ARE signaling in vitro and in vivo, Oxid. Med Cell Longev. 2019 (2019) 8564681.
[51] X. Fang, X. Zhong, G. Yu, S. Shao, Q. Yang, Vascular protective effects of KLF2 on Abeta-induced toxicity: Implications for Alzheimer's disease, Brain Res 2017 (1663) 174–183.
[52] J. Maity, M. Deb, C. Greene, H. Das, KLF2 regulates dental pulp-derived stem cell differentiation through the induction of mitophagy and altering mitochondrial metabolism, Redox Biol. 36 (2020), 101622.
[53] A.B. Malpartida, M. Williamson, D.P. Narendra, R. Wade-Martins, B.J. Ryan, Mitochondrial Dysfunction and Mitophagy in Parkinson's Disease: From Mechanism to Therapy, Trends Biochem Sci. 46 (4) (2021) 329–343.
[54] W.S. el-Deiry, T. Tokino, V.E. Velculescu, D.B. Levy, R. Parsons, J.M. Trent, D. Lin, W.E. Mercer, K.W. Kinzler, B. Vogelstein, WAF1, a potential mediator of p53 tumor suppression, Cell 75 (4) (1993) 817–825.
[55] D.H. Ho, H. Kim, J. Kim, H. Sim, H. Ahn, J. Kim, H. Seo, K.C. Chung, B.J. Park, I. Son, W. Seol, Leucine-Rich Repeat Kinase 2 (LRRK2) phosphorylates p53 and induces p21(WAF1/CIP1) expression, Mol. Brain 8 (2015) 54.
[56] A. Suzuki, Y. Tsutomi, K. Akahane, T. Araki, M. Miura, Resistance to Fas-mediated apoptosis: activation of caspase 3 is regulated by cell cycle regulator p21WAF1 and IAP gene family ILP, Oncogene 17 (8) (1998) 931–939.
[57] S. Kihara, S. Hayashi, S. Hashimoto, N. Kanzaki, K. Takayama, T. Matsumoto, N. Chinzei, K. Iwasa, M. Haneda, K. Takeuchi, K. Nishida, R. Kuroda, Cyclin-Dependent kinase inhibitor-1-deficient mice are susceptible to osteoarthritis associated with enhanced inflammation, J. Bone Min. Res 32 (5) (2017) 991–1001.